OPTIMAL DESIGN OF A SEMI-ACTIVE BRACING MECHANISM

M. Mohebbi[*, †] and S. Bakhshinezhad
Faculty of Technical and Engineering, University of Mohaghegh Ardabili, 56199-11367, Ardabil, Iran

ABSTRACT

The semi-active bracing system locks or unlocks the stand-by braces in an on-off mode utilizing a variable stiffness device (VSD). In this paper, the optimal design of a semi-active bracing mechanism and evaluating its performance in mitigating structural vibration under seismic loading have been studied. The optimal stiffness values of the semi-active braces have been determined by solving two optimization problems including minimizing the maximum acceleration and also minimizing the maximum inter-story drift by imposing a constraint on the maximum acceleration. The genetic algorithm (GA) has been applied to solve the optimization problems. To illustrate the design procedure, an eight-story linear shear frame under earthquake record has been considered and the optimal semi-active braces have been designed. In addition, to assess the performance of optimal bracing system under other records which are different from design record in terms of intensity and frequency content, the structure equipped with optimally designed semi-active braces has been tested under several ground motion records. The results show that the optimal semi-active bracing system has simultaneously reduced different responses of the structure although the acceleration reduction has mainly been less compared to the drift reduction.

1. INTRODUCTION

Over the past few decades, structural control systems under dynamic forces have attracted the attention of many researchers. A semi-active vibration control system comprises the advantages of active and passive control systems simultaneously [1]. Semi-active control

---

[*]Corresponding author: Faculty of Technical and Engineering, University of Mohaghegh Ardabili, 56199-11367, Ardabil, Iran
[†]E-mail address: mohebbi@uma.ac.ir (M. Mohebbi)

systems reduce the structural responses by changing the stiffness or damping parameters.

Different mechanisms have been utilized for semi-active control with variable stiffness such as bracing mechanisms with variable stiffness which was initially proposed by Kobori *et al* [2]. They developed the first semi-active bracing system in the construction of the three-story building of Kajima Research Institute in Japan. This mechanism had been called as active variable stiffness (AVS); however, because of low energy requirement and also not need to apply external force directly into the structure, it is classified as a semi-active control system. In this mechanism, the control system locks or unlocks the stand-by braces based on the appropriate control algorithm at each time step. When the brace is locked, it acts as a structural member and its stiffness will be added to stiffness of the structure. Otherwise, when the brace is unlocked, the structural stiffness has to be supplied by the other structural members. A variable stiffness device (VSD) which is a semi-active hydraulic device is installed between Chevron braces and the beam of the upper floor and operates in an on-off mode.

Furthermore, another semi-active bracing mechanism has been suggested which in this mechanism for modifying the stiffness of the system a resettable semi-active stiffness damper has been used [3,4]. A full-scale prototype of this mechanism has been built and tested by the means of a shaking table by Yang et al. [5] at the University of California. The mentioned semi-active device could also be incorporated in semi-active tuned mass damper mechanisms in addition to semi-active bracing mechanisms [6]. Golafshani et al [7] proposed an alternative variable stiffness bracing mechanism that implements a ribbed bracing system. In this mechanism, the braces do not work in the pressure phase, and as a result, the buckling of the braces is prevented and the ultimate capacities of the braces can be completed. Nagarajaiah and Mate [8] developed semi-active independent variable stiffness (SAIVS) device which provides the ability to modify the stiffness of the braces continuously and steadily. The SAIVS mechanical device consists of four springs connected in a rhombus-shaped geometry, and by changing the relative angle between the springs, the stiffness of the system can be changed instantaneously and continuously between the upper and lower limits. However, due to the large space limitation, this semi-active variable stiffness technique has recently been used in smart base isolation systems [9,10], as well as semi-active tuned mass damper mechanisms [11,12]. It is not applicable in the semi-active bracing system.

In addition, various researches have been conducted to improve the effectiveness of control algorithms in the field of semi-active bracing mechanisms. One of the effective algorithms in controlling structural vibrations by using semi-active bracing systems is the feed-forward method, which decides to lock or unlock the bracing system based on the frequency content of the input vibration. Since the stiffness and subsequently the frequency of the structure varies with the locking and unlocking of the bracing system, at each time step the locked bracing arrangement is selected in such a way that the frequency of the structure has the maximum difference from the dominant excitation frequency. As a result, a non-resonant state is created in the controlled system [13-15]. One of the other control algorithms proposed by Yamada and Kobori [16] is based on processing the response of the structure under the input vibration in the current step and then estimating the subsequent responses for different possible configurations of braces based on the responses of the current step. Then, the state which minimizes the input energy is selected; and immediately for the next time

step, on-off elements are set up. Numerical simulation results under harmonic and earthquake excitations show that despite the reduction of inter-story drift ratios, the maximum acceleration of the structure has increased as a result of impacts caused by sudden changes in the stiffness of the structure. Yang et al. [17] proposed a control algorithm based on sliding mode control and concluded that although this algorithm can significantly reduce the inter-story drift ratios by semi-active variable stiffness, the maximum acceleration of the structure increases significantly.

Some algorithms are based on the motion parameters of the system in addition to some expertise and engineering judgments. The control algorithm introduced here as AVS, proposed by Kamegata and Kobori [18], is based on locking the bracing mechanism under the condition that the displacement and velocity values of a story are both positive or both negative, otherwise the brace is in the unlocked position. In another control algorithm introduced by Inaudi and Hayen [19] and called here as IH control, the bracing mechanism is always locked except for situations where the displacement direction changes or the displacement reaches its maximum value.

Hejazi *et al* [20] designed the semi-active bracing mechanism under earthquake vibrations using the genetic algorithm (GA). In their study, the design variables were the stiffness index of each floor consisting of the stiffness of the structure and the braces, and the objective function of the optimization problem was minimizing the sum of displacement of stories. The results showed an acceptable reduction in the displacements of structure equipped with optimal semi-active bracing mechanism under earthquake vibrations. In this research, the focus was only on reducing the displacement, and controlling other structural responses, which have been known as limiting factors in application of semi-active bracing system in previous researches, has not been considered.

In previous studies in the field of semi-active bracing mechanisms with variable stiffness, mainly various algorithms and mechanisms have been introduced and their efficiency has been investigated. In many theoretical and experimental studies, it has been found that the semi-active control mechanism has a satisfactory ability to reduce displacement and inter-story drift, while there is no such certainty on reducing the acceleration of the structure. It has been observed that in some cases, using this mechanism has led to a significant increase in the acceleration of structures. This significant increase in acceleration is due to the sudden and immediate change in braces stiffness that applies pulse-like loads to the structure.

To overcome the shortcomings of the previous studies, this study attempts to propose a method for the optimal design of the semi-active bracing mechanism under earthquake vibration with the aim of reducing the inter-story drift as a safety criterion and acceleration as a residents' convenience criterion. For this purpose, two optimization problems have been defined and solved using the genetic algorithm. In the first, the objective function is minimizing the maximum acceleration of the structure, and in the second, the objective function has been defined as the minimization of the maximum inter-story drift while a constraint is applied on the maximum acceleration of the structure. Moreover, the efficiency of the optimally designed mechanisms under several testing near-field earthquakes which are different from the design record in terms of the intensity and frequency content, has been evaluated.

2. SEMI-ACTIVE BRACING MECHANISM

The semi-active bracing mechanism, originally introduced by Kobori et al [2], controls the vibration of the structure by changing the stiffness of the structure in each story. This mechanism was displayed schematically in Fig. 1; where, k_{b1}, k_{b2}, ... and k_{bn} are the stiffness of the braces installed in the first to the nth stories. These braces are locked or unlocked at each time step based on the semi-active control algorithm command.
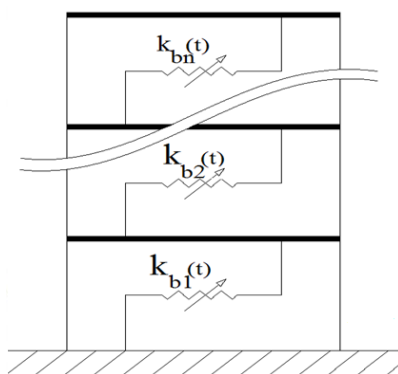
Figure 1. Schematic view of the structure with semi-active bracing mechanism

This mechanism has a variable stiffness device, VSD, which consists of a variable orifice damper to lock and unlock the braces. Fig. 2 shows the VSD device located between beam and diagonal brace. The VSD includes a balanced hydraulic cylinder, a dual piston, a normally closed solenoid valve and a tube connecting the two cylinder chambers together. The energy consumption per application of device is 20 watts. Once the valve is open, the fluid flows freely, the piston moves in the cylinder without damping and the connection between the brace and the beam is broken; so, the stiffness of the braces cannot be added to the stiffness of the structure. When the valve is closed, the fluid cannot flow, the piston cannot move inside the cylinder and the connection between the brace and the beam is effectively locked; thus, the stiffness of braces can be added to the stiffness of the structure. By connecting the device to the bracing system, the control system would be able to change the stiffness of the structure at each time.
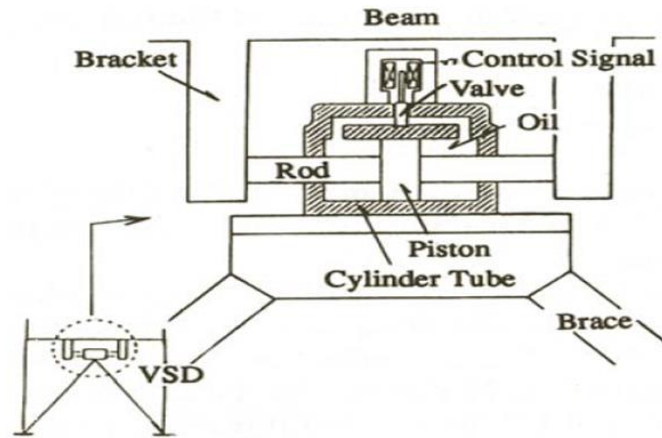
Figure 2. Variable stiffness device attached to the brace [2]

2.1 Equation of motion of structure equipped with semi-active bracing mechanism
Considering a n-story linear shear frame including the semi-active bracing system in all stories and subjected to ground acceleration of $\ddot{x}_g$, the system's equation of motion in matrix form is written as follows:

$$\mathbf{M}\ddot{\mathbf{X}}(t) + \mathbf{C}\dot{\mathbf{X}}(t) + \mathbf{K}\mathbf{X}(t) = \mathbf{U}_{SA}(t) + \mathbf{M}\mathbf{e}\ddot{x}_g \tag{1}$$

where $\mathbf{M}$, $\mathbf{C}$ and $\mathbf{K}$ are respectively the mass, damping and stiffness matrices of the main structure which can be determined using Eqs. 2-4 in which m_i, c_i and k_i are the mass, damping and stiffness of ith-story. $\mathbf{X}$ represents the displacement vector relative to the ground as defined in Eq. 5 and $\mathbf{e}$ is the ground acceleration transformation vector defined as Eq. 6.

$$\mathbf{M} = diag\left[m_1,\, m_2,\, ...,m_{n-1},\, m_n\right] \tag{2}$$

$$\mathbf{C} = \begin{bmatrix} c_1 + c_2 & -c_2 & \cdots & 0 & 0 \\ -c_2 & c_2 + c_3 & \cdots & 0 & 0 \\ \vdots & \vdots & \ddots & \vdots & \vdots \\ 0 & 0 & \cdots & c_{n-1} + c_n & -c_n \\ 0 & 0 & \cdots & -c_n & c_n \end{bmatrix} \tag{3}$$

$$\mathbf{K} = \begin{bmatrix} k_1 + k_2 & -k_2 & \cdots & 0 & 0 \\ -k_2 & k_2 + k_3 & \cdots & 0 & 0 \\ \vdots & \vdots & \ddots & \vdots & \vdots \\ 0 & 0 & \cdots & k_{n-1} + k_n & -k_n \\ 0 & 0 & \cdots & -k_n & k_n \end{bmatrix} \tag{4}$$

$$\mathbf{X} = \left[x_1,\, x_2,\, ...,x_{n-1},\, x_n\right]^T \tag{5}$$

$$\mathbf{e} = \begin{bmatrix} -1, -1, \ldots, -1 \end{bmatrix}^T \tag{6}$$

Also, in Equation (1), $\mathbf{U}_{SA}$ is the vector of semi-active control force which is determined using Eq. 7.

$$\mathbf{U}_{SA}(t) = -\mathbf{K}_{SA}(t) \times \mathbf{X}(t) \tag{7}$$

in which $\mathbf{K}_{SA}$ is the stiffness matrix of semi-active system derived by assembling the stiffness of braces in different stories as Eq. 8.

$$\mathbf{K}_{SA}(t) = \begin{bmatrix} k_{b1}(t) + k_{b2}(t) & -k_{b2}(t) & \cdots & 0 & 0 \\ -k_{b2}(t) & k_{b2}(t) + k_{b3}(t) & \cdots & 0 & 0 \\ \vdots & \vdots & \ddots & \vdots & \vdots \\ 0 & 0 & \cdots & k_{b(n-1)}(t) + k_{bn}(t) & -k_{bn}(t) \\ 0 & 0 & \cdots & -k_{bn}(t) & k_{bn}(t) \end{bmatrix} \tag{8}$$

where k_{b1}, k_{b2}, ... and k_{bn} are respectively the braces stiffness of stories 1, 2…, and n which are determined at each time step based on the semi-active control algorithm. In this paper, Newmark's numerical method [21,22] is used to solve the system's equation of motion.

3. THE SEMI-ACTIVE CONTROL ALGORITHMS

Semi-active bracing system has the capability of locking and unlocking by semi-active VSD. The stiffness of control mechanism is switched in an on-off mode at each time step using an appropriate control algorithm. In this study, two effective control algorithms developed in previous researches have been comprehensively introduced and applied to control the semi-active bracing mechanisms.

3.1 AVS control law
Kamagata and Kobori [18] for the first semi-active bracing mechanism called active variable stiffness, AVS, have employed several control algorithms. One of these algorithms which is referred here as AVS is based on the following equations.

$$\begin{cases} u_i(k) \times \dot{u}_i(k) \geq 0 & \Rightarrow \quad \textit{close the bracing} \\ u_i(k) \times \dot{u}_i(k) < 0 & \Rightarrow \quad \textit{open the bracing} \end{cases} \tag{9}$$

where $u_i(k)$ and $\dot{u}_i(k)$ are the inter-story drift and velocity of the ith-story of the structure at k^{th} time step.

When the inter-story drift and velocity of the structure are both positive or negative ($u_i(k) \times \dot{u}_i(k) \geq 0$), the braces must be locked. As well as, when the inter-story drift and velocity of the structure are in the opposite directions, the braces must be opened. In other

words, as long as the elastic energy is increasing, the braces should be locked, otherwise they should be unlocked. The flowchart of the on-off AVS control algorithm and the theoretical hysteresis behavior of the semi-active brace in one cycle have been shown in Figs. 3-4, respectively.

Start

$Inputs: u_i(k), u_i(k-1), \dot{u}_i(k)$

$\Delta u_i = u_i(k) - u_i(k-1)$

$u_i(k) \times \dot{u}_i(k) \geq 0$ — Yes →

close the bracing
$(\Delta u_b)_i = \Delta u_i$
$(u_b)_i(k) = (u_b)_i(k-1) + (\Delta u_b)_i$
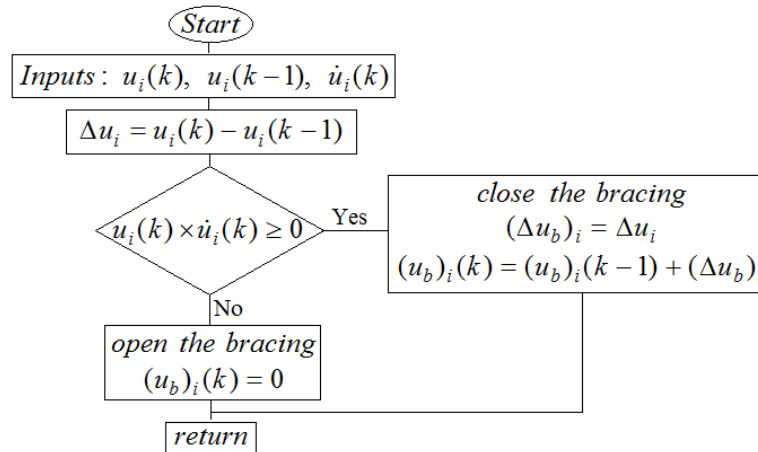
No

open the bracing
$(u_b)_i(k) = 0$

return

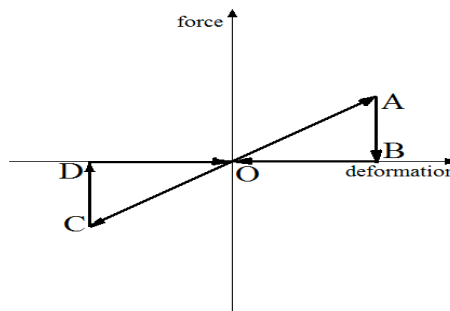Figure 3. Flowchart of AVS control algorithm

Figure 4. The theoretical hysteresis behavior of bracing system in AVS control algorithm

According to Fig. 3, the three input parameters required for the AVS algorithm are the inter-story drift value at time steps (k) and (k-1) as well as the inter-story velocity value at time step (k). At each time step in each story, first the variation of the frame drift (Δu) is calculated. Then, if the product of the inter-story drift and velocity is positive, the brace is locked and the variation of the brace relative displacement is assumed equal to the variation of frame drift ($\Delta u_b = \Delta u$). In this case, the new brace relative displacement $(u_b)_i$ is obtained from the sum of the brace relative displacement in pervious step and the calculated variation of brace relative displacement. On the other hand, if the product of the inter-story drift and velocity of the frame is negative, the brace is unlocked and the brace relative displacement is considered to be zero.

3.2 IH control law
The IH control algorithm was first proposed by Inaudi and Hayen [19]. In this control

algorithm, the bracing system is always in active mode except when the inter-story drift of the frame reaches the maximum value and wants to change its direction. At this moment, the bracing system is unlocked immediately and the brace relative displacement becomes zero. This control algorithm is presented in the following equations:

$$\begin{cases} \dot{u}_i(k-1)\times\dot{u}_i(k)\geq 0 & \Rightarrow \quad close\ the\ bracing \\ \dot{u}_i(k-1)\times\dot{u}_i(k)<0 & \Rightarrow \quad open\ the\ bracing \end{cases} \tag{10}$$

The flowchart of the on-off IH control algorithm as well as the theoretical hysteresis behavior of the bracing system are respectively displayed in Figs. 5-6. In control algorithm of IH, four input parameters are required including inter-story drift and velocity values in two successive time steps.
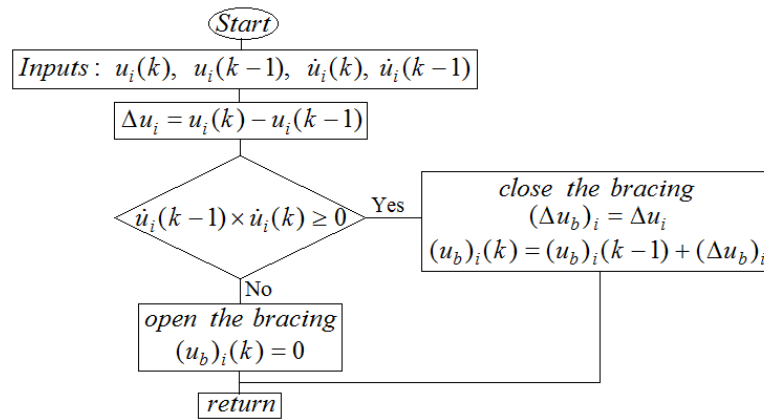
Figure 5. Flowchart of IH control algorithm

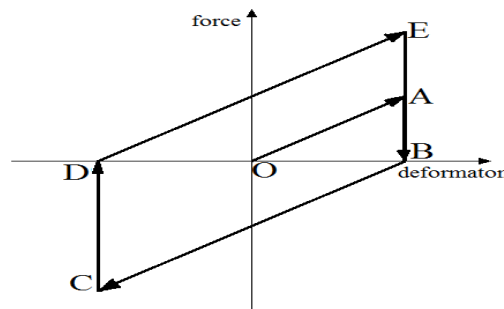Figure 6. The theoretical hysteresis behavior of bracing system in IH control algorithm

4. OPTIMAL DESIGN OF SEMI-ACTIVE BRACING SYSTEM

In this paper, the optimal value of the design parameters of the semi-active bracing system, including the stiffness of the braces in each floor, are determined based on the minimization of an objective function. The purpose of using the semi-active bracing system is to reduce

the structure's vibrations, as a result to limit the structure's responses. For this purpose, for optimal design of the semi-active braces two single objective optimization problems are defined and solved using GA.

4.1 Case A

In this case, the objective function has been defined as the minimization of the maximum acceleration of the structure. By considering t_0 and t_f as the initial and final time step of analysis, the optimization problem is defined as follows:

$$Find \qquad (k_b)_i \qquad (i = 1, 2, ..., n) \tag{11}$$

$$Minimize \qquad F(T) = \alpha \, \ddot{x}_{max} \tag{12}$$

$$Subject\,to \qquad (k_{b\,min})_i < (k_b)_i < (k_{b\,max})_i \tag{13}$$

where α is a constant coefficient, n is the number of stories and k_b is the stiffness of the brace. $\ddot{x}_{max}$ represents the maximum acceleration determined as Eq. 14.

$$\ddot{x}_{max} = Max(|\ddot{x}_k(i)|) , \qquad i = 1, 2, ..., n \quad , k = 1, 2, ..., k_{max} \tag{14}$$

Assuming time step as Δt, the total number of time steps is equal to:

$$k_{max} = (t_f - t_0) / \Delta t \tag{15}$$

also, $k_{b\,min}$ and $k_{b\,max}$ are respectively the lower and upper limits of the braces stiffness values which could be defined by the designer.

4.2 Case B

In the second optimization problem, the objective function has been defined as the minimization of the maximum inter-story drift of the structure while applying a constraint on its maximum acceleration. In this case, the optimization problem is defined as follows:

$$Find \qquad (k_b)_i \qquad (i = 1, 2, ..., n) \tag{16}$$

$$Minimize \qquad F(T) = \beta \, u_{max} \tag{17}$$

$$Subject\,to \qquad \ddot{x}_{max} \leq \lambda \, \ddot{x}_{max,\,uncontrolled} \tag{18}$$

Therefore, in this case there is a constrained optimization problem. The constraint is considered as not exceeding the maximum acceleration of the structure from a percentage of the maximum acceleration of the uncontrolled structure. The allowable maximum acceleration of the controlled structure is determined using λ coefficient. By using the penalty method [23], this constrained optimization problem is transformed into an unconstrained optimization problem by defining a new objective function. The substituted

unconstrained optimization problem can be written as follows:

$$Find \qquad (k_b)_i \tag{19}$$

$$Minimize \qquad F(T) = \beta u_{max} + \gamma \max[0, g_1] \tag{20}$$

$$g_1 = \frac{\ddot{x}_{max}}{\lambda \ddot{x}_{max, uncontrolled}} - 1$$

where β, γ and λ are constant coefficients and u_{max} is the maximum inter-story drift of the structure that is determined using Eq. 21.

$$u_{max} = Max(|u_k(i)|), \qquad i = 1, 2, ..., n \quad , k = 1, 2, ..., k_{max} \tag{21}$$

5. GENETIC ALGORITHM

Genetic algorithm, GA, first proposed by Holland [23], is an effective computational method for solving different linear and nonlinear optimization problems, based on the mechanism of natural genetics processes. In GA, initial population of individuals is created randomly and improved repeatedly. At each generation, the fitness of each individual is calculated and highly fit individuals are used to generate the next population. The main operators of GA are selection, crossover and mutation [24].

In this paper, for selecting the individuals for mating the stochastic universal sampling method [25] has been used, where the probability of selecting an individual is as follows:

$$P(\mathbf{x}_i) = \frac{F(\mathbf{x}_i)}{\sum_{i=1}^{N_{ind}} F(\mathbf{x}_i)}, \qquad i = 1, 2, ..., N_{ind} \tag{22}$$

where $F(\mathbf{x}_i)$ = fitness of chromosome $\mathbf{x}_i$, $P(\mathbf{x}_i)$ = probability of selection of $\mathbf{x}_i$ and N_{ind} = number of individuals.

The newborns are generated by using crossover operator in a random form based on selected parents' chromosomes as follows:

$$G = P_1 + \mu(P_2 - P_1) \tag{23}$$

where G= the value of newborn gene, P_1 and P_2 are the parent chromosomes genes and μ is a scale factor that chosen randomly in the range of [-0.25, 1.25] typically. The mutation operator is used to help GA to escape from local optimal point and to guarantee searching all individuals. Considering mutation rate equal to η, the number of mutated genes is determined using Eq. 24.

$$N_{mutated} = \eta \times N_{var} \times N_{new} \tag{24}$$

where N_{var} =number of variables and N_{new} = number of newborns.

GA has been used successfully to solve various optimization problems in civil engineering [26-28] as well as structural control systems such as designing smart base isolation [29], semi-active tuned mass dampers [30, 31], optimal placement of MR dampers [32], optimal design of semi active control for adjacent buildings connected by MR damper [33] and using multi-objective genetic algorithm for semi-active fuzzy control of a wind-excited tall building [34].

6. ANALYTICAL STUDIES

In this section a numerical example has been presented to explain the optimal design procedure of semi-active bracing mechanism under earthquake excitation. An eight-story linear shear frame has been selected for numerical analysis where its semi-active braces have been designed according to the optimization strategies presented in section 4. The optimal values of stiffness for the semi-active braces were determined using the genetic algorithm technique. Moreover, the effectiveness of optimally designed mechanisms and the proposed method have been examined under near-field earthquakes and the responses of controlled and uncontrolled frames were compared. The eight-story frame has the uniform parameters in all stories as presented in Table 1. The characteristics of the test near-field earthquakes were reported in Table 2.

Table 1. Structural parameters of the frame

Parameter	Value
m(ton)	345.6
k(MN/m)	680
c(kN.s/m)	734

Table 2. Characteristics of the test near-field earthquakes

Earthquake Number	Earthquake	Year	Station	PGA (g)	RJB (kM)	Magnitude (M)
1	Cape Mendocino	1992	Petrolia	0.591	0.0	7.1
2	Chi-Chi	1999	CHY080	0.809	0.11	7.62
3	Coalinga	1983	Anticline Ridge Pad	0.486	1.41	5.09
4	Imperial Valley	1940	El Centro Array #9	0.281	6.09	6.95
5	Kobe	1995	KJMA	0.834	0.94	6.9
6	Loma Prieta	1989	BRAN	0.456	3.85	6.93
7	Northridge	1994	Arleta – Nordhoff Fire Sta	0.345	3.3	6.69
8	Parkfield	2004	PARKFIELD-MIDDLE MOUNTAIN	0.184	0.61	6.0
9	San Fernando	1971	Lake Hughes #12	0.194	13.99	6.61
10	Superstition Hills	1987	Superstition Mtn Camera	0.582	5.61	6.54

6.1 Comparative results
In the eight-story shear frame, braces are installed in all stories. It is obvious that the values

of braces stiffness affect the efficiency of the control system. Therefore, in the first step, to perform a sensitivity analysis on the effect of the bracing system stiffness values on the structural response, different values for the stiffness of the bracing system have been considered. The ratio of bracing stiffness value to the main structure stiffness value is defined as Eq. 25.

$$r = \frac{k_b}{k_s} \tag{25}$$

where k_b is the stiffness of the bracing system and k_s is the stiffness of the main structure.

For evaluating the performance of the semi-active bracing mechanism, different stiffness ratios have been assumed. As an example, the responses of the uncontrolled frame as well as controlled frame with the passive and semi-active bracing systems, under the El-Centro record have been presented in Figs. 7-9, respectively for two control algorithms IH and AVS.
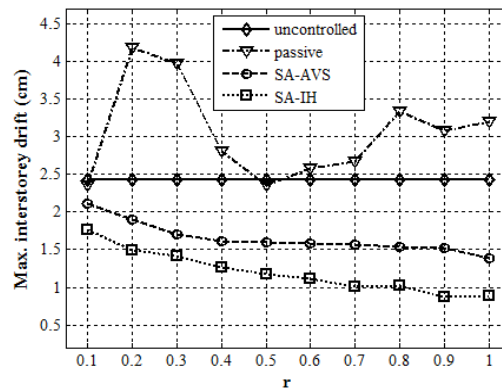

Figure 7. Maximum drift of uncontrolled and controlled frames under the El-Centro record
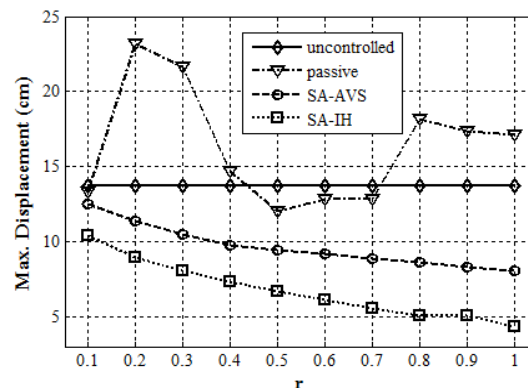

Figure 8. Maximum displacement of uncontrolled and controlled frames under the El-Centro record
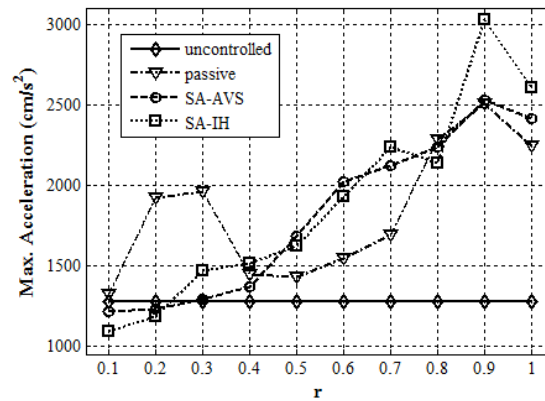
Figure 9. Maximum acceleration of uncontrolled and controlled frames under the El-Centro record

The results show that the performance of the control system strongly depends on the stiffness ratio. It can also be concluded that the semi-active control system has a higher ability to reduce the drift and displacement of the structure, especially in samples with a higher stiffness ratio.

Regarding the acceleration of the structure, it can be seen that the increase in the stiffness ratio, r, increases the acceleration of the structure. Changing the stiffness of the bracing system at any time step and as a result applying pulse-like forces to the structure are considered as a technical weakness that limits application of this control system. It can be seen in Fig. 9 that as the stiffness ratio decreases, the increase in acceleration decreases, while in the stiffness ratio of 0.1 and 0.2, the semi-active control system can even reduce the acceleration. This range for stiffness ratio can be used for this system, but in this case the reduction in drift is not significant. An increase in acceleration was observed under most earthquake records. Therefore, the optimal design of bracing stiffness, especially with different stiffness values for each floor, can provide a semi-active mechanism with the ability to control all the responses of structures.

6.2 Optimal design of semi-active bracing system

In this section, optimal semi-active braces are designed using two control algorithms, AVS and IH, and their performance is evaluated. One semi-active brace with the stiffness of $(k_b)_i$ is considered in i^{th}-story. The El-Centro earthquake has been selected as the design record. The value of stiffness of braces are considered as the design variable of both the previously mentioned optimization problems and the optimal values are determined using GA. The domain of braces stiffness value (k_b) in solving the optimization problem is considered as Eq. 26.

$$k_b \in \left(0.01 k_s, k_s\right) \tag{26}$$

For the eight-story frame, there are eight variables ($k_{b1}, k_{b2}, k_{b3}, k_{b4}, k_{b5}, k_{b6}, k_{b7}, k_{b8}$).

6.2.1 Design of the semi-active bracing system based on Case A
In this case, the semi-active control system has been designed based on minimizing the maximum acceleration of structure for both control algorithms. The value of α in Eq. 12 has been considered as follows:

$$\alpha = \frac{1}{\ddot{x}_{max\,uncontrolled}} = \frac{1}{1272.8} \qquad (27)$$

The optimization problem defined in Eqs. 11-13 have been solved using the genetic algorithm for several times and the optimal values of semi-active braces stiffness have been presented in the Table 3. Also, to compare the performance of the passive braces, the optimal values of passive braces stiffness have been also reported in Table 3.

Table 3. Optimal stiffness of the bracing system

Story No.	k_b(MN/m)		
	SA brace (IH-*Case A*)	SA brace (AVS-*Case A*)	Passive brace
1	1.494042E8	5.264563E7	1.380013E7
2	8.582074E7	3.446551E7	1.393056E7
3	4.973961E7	4.985940E7	1.36E7
4	9.008436E7	7.712244E7	1.405353E7
5	1.527280E8	1.413121E8	2.111817E8
6	1.662678E8	1.905382E8	6.772513E8
7	2.280703E8	1.918546E8	2.155746E8
8	2.855160E8	2.621536E8	6.776289E8

For optimal passive and semi-active bracing mechanisms, the response of controlled frames as well as uncontrolled frame have been given in Table 4.

Table 4. Maximum responses of uncontrolled and controlled frames

Mechanism	Drift (cm)	Disp (cm)	Acc (cm/s^2)
Uncontrolled	2.42	13.74	1272.8
Passive brace	2.77	12.30	**955.6**
SA brace (AVS- *Case A*)	2.33	11.89	1012.4
SA brace (IH- *Case A*)	**1.69**	**8.87**	986.1

The results show that although using the passive bracing system causes a greater reduction in the structure's acceleration, the maximum drift of controlled structure has increased. On the other hand, from the results it has been found that the application of the semi-active control system, especially based on the IH algorithm, effectively reduces the responses of the structure, so that for the IH algorithm, the maximum drift, displacement, and acceleration have reduced by approximately 30%, 35%, and 23%, respectively. Therefore, it is clear that the optimal semi-active bracing has the ability to reduce various

responses of the structure simultaneously, although it has been more effective in reducing drift and displacement compared to acceleration.

6.2.2 Design of the semi-active bracing system based on Case B
In this section for both control algorithms IH and AVS, the semi-active bracing system has been designed based on minimizing the maximum drift of the structure while a constraint is applied on its maximum acceleration. In the optimization problem defined in Eqs. 19-20, β has been considered as follows:

$$\beta = \frac{1}{u_{max\,uncontrolled}} = \frac{1}{2.42} \tag{28}$$

Also, the value of γ has been considered equal to 100. Three values of 1, 0.9 and 0.8 have been considered for λ, which are respectively equivalent to no reduction, 10% and 20% reduction in the maximum acceleration of the uncontrolled frame. Also, by assuming the value of this coefficient to be infinite, the minimization of the maximum drift of the structure without constraint on the acceleration of the structure has been considered. The optimal stiffness values of passive and semi-active braces are presented in Table 5.

Table 5. Optimal stiffness of the bracing system

| Story No. | k_b (MN/m) | | | | | | | | |
| | Passive brace | | | SA brace (AVS - *Case B*) | | | SA brace (IH - *Case B*) | | |
	$\lambda = 0.8$	$\lambda = 0.9$	$\lambda = 1$	$\lambda = 0.8$	$\lambda = 0.9$	$\lambda = 1$	$\lambda = 0.8$	$\lambda = 0.9$	$\lambda = 1$
1	6.357E7	1.474E8	2.800E8	1.903E8	2.552E8	2.275E8	6.213E7	1.659E8	1.935E8
2	3.960E7	1.208E8	1.769E8	6.460E7	1.494E8	1.833E8	2.002E7	1.157E8	1.530E8
3	5.678E7	1.598E8	2.572E8	7.611E7	1.660E8	1.900E8	7328749	3.932E7	7.842E7
4	7.513E7	1.450E8	1.931E8	1.150E8	2.302E8	2.169E8	7289976	1.466E7	1.956E7
5	1.340E8	1.886E8	1.520E8	1.910E8	3.239E8	1.604E8	2.404E8	1.415E8	1.556E7
6	1.726E8	2.570E8	2.827E8	1.588E8	2.737E8	6.375E7	2.862E8	2.190E8	3.630E7
7	1.836E8	1.517E8	1.387E8	2.490E8	3.817E8	2.739E8	3.194E8	1.699E8	2.075E8
8	2.714E8	3.110E8	2.831E8	1.979E8	1.991E7	3.642E8	3.137E8	2.135E8	1.766E8

The responses of the frames equipped with the passive and semi-active bracing systems designed based on *Case B* have been reported in Table 6 and Fig. 10 under the El-Centro record. It can be said that by changing the value of λ, the priority of reducing drift and acceleration can be adjusted by the designer. Because more reduction of one response can lead to less reduction of another response. Also, the results show that the design of semi-active braces based on *Case B* has led to a more effective reduction in the maximum drift, especially by using the IH algorithm, which it is possible to reduce the maximum drift by 66% for $\lambda = \infty$ and 43% for $\lambda = 1$.

Table 6. Maximum responses of uncontrolled and controlled frames

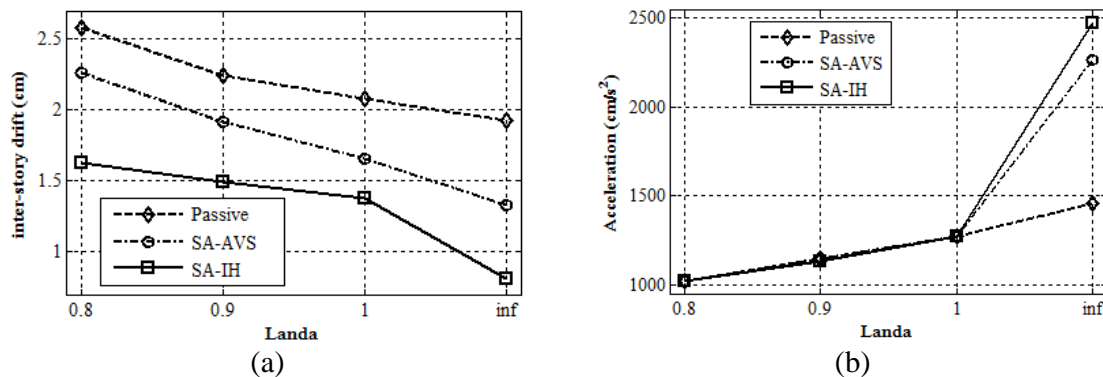| Mechanism		Drift (cm)	Disp (cm)	Acc. (cm/s^2)
Uncontrolled		2.42	13.74	1272.8
Passive brace	$\lambda = \infty$	**1.92**	**12.14**	1455.4
	$\lambda = 1$	2.08	12.99	1272.1
	$\lambda = 0.9$	2.25	12.67	1144
	$\lambda = 0.8$	2.58	12.45	**1017.9**
SA brace (AVS-*Case B*)	$\lambda = \infty$	**1.33**	**8.89**	2263.1
	$\lambda = 1$	1.66	10.33	1272.8
	$\lambda = 0.9$	1.91	10.88	1145.5
	$\lambda = 0.8$	2.26	11.91	**1018.1**
SA brace (IH- *Case B*)	$\lambda = \infty$	**0.81**	**5.37**	2469.6
	$\lambda = 1$	1.38	8.30	1272.6
	$\lambda = 0.9$	1.49	7.73	1133.9
	$\lambda = 0.8$	1.63	8.80	**1017.9**

Figure 10. Maximum (a) drift and (b) acceleration of controlled frame under the El-Centro record

6.3 Performance of semi-active bracing system under near-field records

To evaluate the effectiveness of the optimal semi-active bracing mechanism under different earthquake records, the structure equipped with the optimal bracing mechanisms subjected to the records presented in Table (2), which are different in terms of intensity and frequency content from the design earthquake. The maximum responses of uncontrolled and controlled frames have been reported in Table 7. From the results, it is clear that drift and displacement of the structure have decreased under all test earthquakes. While under some of earthquakes, the value of the maximum acceleration has increased compared to the uncontrolled structure, but the average value of the decrease and increase of the maximum acceleration under the test earthquakes has been decreasing. For example, for the semi-active bracing system designed based on *Case A* using the IH control algorithm, the average reduction in the maximum drift and displacement has been about 48% and 43%, respectively, while the average reduction in the maximum acceleration has been about 10%. For *Case B* using the

IH control algorithm with λ=0.8, the average reduction in maximum acceleration, drift and displacement was about 4%, 46% and 45%, respectively. Therefore, it can be said that the optimal semi-active braces have the ability to reduce different responses of the structure simultaneously although the acceleration reduction under test earthquakes was less compared to drift reduction.

Table 7. Response of the uncontrolled and controlled frames under near-field earthquakes

Earthquake	Uncontrolled			AVS-*Case A*			AVS-*Case B* ($\lambda = 0.8$)			IH-*Case A*			IH-*Case B* ($\lambda = 0.8$)		
	Drift (cm)	Disp. (cm)	Acc. (cm/s^2)	Drift (cm)	Disp. (cm)	Acc. (cm/s^2)	Drift (cm)	Disp. (cm)	Acc. (cm/s^2)	Drift (cm)	Disp. (cm)	Acc. (cm/s^2)	Drift (cm)	Disp. (cm)	Acc. (cm/s^2)
El-Centro (design record)	2.42	13.74	1272.8	2.33	11.89	1012.4	2.26	11.91	1018.1	1.69	8.87	**986.1**	**1.63**	**8.80**	1017.9
Cape Mendocino	7.91	43.09	3276.9	6.53	32.93	3307.5	6.60	32.11	3377.9	**3.86**	20.07	**2871.1**	3.92	**18.88**	3030.2
Chi-Chi	12.22	66.30	4201.9	8.19	40.23	3896.3	7.96	39.76	**3337.5**	**5.77**	31.03	4103.1	5.85	**28.19**	5104.3
Coalinga	1.04	3.13	1146.5	0.82	2.99	1230.9	0.83	2.99	1216	0.53	2.24	**1005.4**	**0.52**	**2.21**	1061.5
Imperial Valley	2.38	13.68	1134.6	1.68	8.89	**784.4**	1.63	8.89	795.2	1.29	6.76	918.2	**1.25**	**6.50**	1035.5
Kobe	8.90	46.88	**3387.6**	7.94	36.99	4276	7.65	36.77	4127.1	**5.03**	26.17	3650.3	5.05	**25.27**	3417.7
Loma Prieta	6.67	34.86	2947.3	4.56	22.88	2675.2	4.36	22.40	**2613**	**2.92**	15.53	2669	3.16	**15.22**	2940.7
Northridge	3.39	17.36	**1283.9**	2.95	14.38	1369.3	2.89	14.31	1363.7	**1.91**	10.86	1556.1	2.00	**9.83**	1730.3
Parkfield	0.84	3.59	545.5	0.72	3.27	504.8	0.72	3.27	**496.9**	0.66	2.82	503.9	**0.64**	**2.81**	559.9
San Fernando	0.34	1.42	298.9	0.26	1.23	264.1	0.26	1.23	263.9	**0.18**	0.98	**248.1**	0.19	**0.97**	252.6
Superstition Hills	4.04	17.54	2433.9	2.82	15.43	1772.6	2.76	15.41	1757.4	1.35	7.46	**1430.1**	**1.27**	**7.03**	1490.1

7. CONCLUSIONS

In this research, the optimal design of the semi-active bracing system has been studied and its performance in reducing the vibration of the structure under earthquake excitation has been evaluated. IH and AVS algorithms have been used as semi-active control algorithms to determine the control signals at each time step to change the bracing stiffness in off-on mode. To design the optimal semi-active bracing system, an optimization-based design method has been proposed that considers the stiffness of braces as design variables and minimizes the structural response as an objective function. Two optimization problems by minimizing the maximum acceleration (*Case A*) and minimizing the maximum drift by imposing a constraint on the maximum acceleration (*Case B*) have been considered and the genetic algorithm (GA) has been used to solve the optimization problems. For numerical simulations, an eight-story shear frame under the El-Centro earthquake has been selected and the optimal semi-active bracing system has been designed using the IH and AVS control algorithms. Also, the optimal passive bracing system was designed for performance comparison. The results showed that the performance of the semi-active bracing system strongly depends on the stiffness ratio. Considering uniform stiffness for braces in different stories, it has been observed that increasing the stiffness ratio leads to further reduction in drift and displacement while the maximum acceleration of the structure increases. Moreover, the results show that by using optimal semi-active bracings for both cases *A* and *B*, the

maximum acceleration, displacement and drift can be reduced simultaneously, although the maximum drift and displacement have reduced more. For example, by applying the semi-active control system based on the IH algorithm in *Case A*, the maximum drift, displacement, and acceleration are reduced by approximately 30%, 35%, and 23%, respectively. Also, the results show that it is possible to achieve an effective reduction in the maximum drift in designing the semi-active braces based on *Case B*, especially by using the IH algorithm which it is possible to reduce the maximum drift by 66% for $\lambda = \infty$ and 43% for $\lambda = 1$. In addition, the evaluation of the performance of the semi-active braces under the test earthquakes shows that this control system has also been effective in reducing the responses of the structure, especially the maximum drift, under the test earthquakes.

REFERENCES

1. Spencer BF, Nagarajaiah S. State of the art of structural control, J *Struc Eng ASCE* 2003, **129**: 845–856.
2. Kobori T, Takahashi M, Nasu T, Niwa N, Ogasawara K. Seismic response-controlled structure with active variable stiffness system, *Earthq Eng Struct Dyn* 1993, **22**: 925–941.
3. Yang JN, Kim J, Agrawal AK. Resetting semiactive stiffness damper for seismic response control, *J Struc Eng ASCE* 2000; **126**: 1427–1433.
4. Jabbari F, Bobrow JE. Vibration suppression with a resettable device, *J Eng Mech ASCE* 2002; **128**: 916–924.
5. Yang JN, Bobrow J, Jabbari F, Leavitt J, Cheng CP, Lin PY. Full-scale experimental verification of resettable semi-active stiffness dampers, *Earthq Eng Struct Dyn* 2007, **36**: 1255–1273.
6. Lin GL, Lin CC, Chen BC, Soong TT. Vibration control performance of tuned mass dampers with resettable variable stiffness, *Eng Struct* 2015, **83**: 187–197.
7. Golafshani AA, Rahani EK, Tabeshpour MR. A new high performance semi-active bracing system, *Eng Struct* 2006, **28**: 1972–1982.
8. Nagarajaiah S, Mate D, Semiactive control of continuously variable stiffness system, *Proc. of 2nd World Conf. Struct. Control* 1988, Kyoto, Japan, **Vol.1**, 397-405.
9. Narasimhan S, Nagarajaiah S. STFT algorithm for semiactive control of base isolated buildings with variable stiffness isolation systems subjected to near fault earthquakes, *Eng Struct* 2005, **27**: 514–523.
10. Nagarajaiah S, Sahasrabudhe S. Seismic response control of smart sliding isolated buildings using variable stiffness systems: experimental and numerical study, *Earthq Eng Struct Dyn* 2006, **35**: 177–197.
11. Nagarajaiah S, Sonmez E. Structures of semiactive variable stiffness multiple tuned mass dampers under harmonic forces, *J Struc Eng ASCE* 2007, **133**: 67–77.
12. Nagarajaiah S. Adaptive passive, semiactive, smart tuned mass dampers: identification and control using empirical mode decomposition, Hilbert transform, and short-term Fourier transform, *Struct Control Health Monit* 2009, **16**: 800–841.
13. Nasu T, Kobori T, Takahashi M, Niwa N, Ogasawa K. Active variable stiffness system with non-resonant control, *Earthq Eng Struct Dyn* 2001, **30**: 1597–1614.
14. Pnevmatikos NG, Kallivokas LF, Gantes CJ. Feed-forward control of active variable stiffness systems for mitigating seismic hazard in structures, *Eng Struct* 2004, **26**: 471–483.

15. Pnevmatikos NG, Gantes CJ. Design and control algorithm for structures equipped with active variable stiffness devices, *Struct Control Health Monit* 2010, **17**: 591–613.

16. Yamada K, Kobori T. Control algorithm for estimating future responses of active variable stiffness structure, *Earthq Eng Struct Dyn* 1995, **24**: 1085–1099.

17. Yang JN, Wu JC, Li Z. Control of seismic-excited buildings using active variable stiffness systems", *Eng Struct* 1996, **18**: 589–596.

18. Kamagata S, Kobori T. Autonomous adaptive control of active variable stiffness systems (AVS) for seismic ground motion, *Proc. of First WCSC* 1994, Los Angeles, **Vol.2**, TA4/33-42

19. Inaudi JA, Hayen JC. Research on variable structure systems in the United States*, Proceedings of the International Post-Smirt Conference Seminar on Seismic Isolation, Passive Energy Dissipation and Control of Structures* 1995, Santiago (Chile), 591-622.

20. Hejazi F, Noorzaei J, Jaafar MS, Thanoon W, Abang Ali AA. Optimization of active variable stiffness system for controlling structural response of a building under earthquake excitation, *J Struc Eng ASCE 2009*, **36**: 235–42.

21. Newmark NM. A method of computation for structural dynamics, *J Eng Mech Div ASCE* 1959, **85**: 67–94.

22. Subbaraj, K., and Dokainish, M.A., (1989) "A survey of direct time-integration methods in computational structural dynamics-II. implicit methods", *Comp Struct*; **32**: 1387-1401.

23. Rao SS. *Engineering Optimization*: Theory and Practice, John Wiley & Sons, 2009

24. Goldberg DE. *Genetic algorithms in search, optimization and machine Learning*, Addison-Wesley Publishing Co., Inc. Reading, Mass,1989.

25. Baker JE, Reducing bias and inefficiency in the selection algorithm *In 2nd International Conference on Genetic Algorithm (ICGA)*1987, Cambridge, MA, USA, 14–21.

26. Moradi M, Bagherieh AR, Esfahani MR. Damage and plasticity of conventional and high - strength concrete part1: statistical optimization using genetic algorithm, *Int J Optim Civil Eng* 2018; 8(1): 77-99. 26.

27. Gholizadeh S, Kamyab R, Dadashi H. Performance-based design optimization of steel moment frames, *Int J Optim Civil Eng* 2013; 3(2): 327-43. 27.

28. Biabani Hamedani K, Kalatjari VR. Structural system reliability-based optimization of truss structures using genetic algorithm, *Int J Optim Civil Eng* 2018; 8(4): 565-86.

29. Mohebbi M, Dadkhah H. Optimal smart isolation system for multiple earthquakes, Int *J Optim Civil Eng* 2019, **9**(1): 19-37.

30. Bakhshinezhad S, Mohebbi M. Fragility curves for structures equipped with optimal SATMDs, *Int J Optim Civil Eng* 2019; **9**(1): 437-455.

31. Bakhshinezhad S, Mohebbi M. Muti-objective optimal design of SATMD including soil-structure interaction using NSGA-II, *Int J Optim Civil Eng* 2020, **10**(3): 391-409.

32. Payandeh-Sani M, Ahmadi-Nedushan B. Optimal placement pf magneto-rheological dampers using NSGA-II based fuzzy control, *Int J Optim Civil Eng* 2023; **13**(2): 189-205.

33. Uz ME, Hadi MNS. Optimal design of semi active control for adjacent buildings connected by MR damper based on integrated fuzzy logic and multi-objective genetic algorithm, *Eng Struct* 2014, **69**: 135-148.

34. Kim HS, Kang JW. Semi-active fuzzy control of a wind-excited tall building using multi-objective genetic algorithm, *Eng Struct* 2012, **41**: 242-257.